MODELING END MILLING WITH RUNOUT

Anna Carla Araujo, Ricardo Rodrigues Alvarez, José Luís Silveira

MODELING END MILLING WITH RUNOUT

Ricardo Rodrigues Alvarez
PEM/ COPPE/ UFRJ – P.O. BOX 68503 – 21945-970 – Rio de Janeiro, RJ, Brazil
gti2000@ufrj.br

Anna Carla Araujo
PEM/ COPPE/ UFRJ – P.O. BOX 68503 – 21945-970 – Rio de Janeiro, RJ, Brazil
annacarla@serv.com.ufrj.br

José Luís Silveira
PEM/ COPPE/ UFRJ – P.O. BOX 68503 – 21945-970 – Rio de Janeiro, RJ, Brazil
jluis@ufrj.br

Abstract. The instantaneous uncut chip thickness and specific cutting forces have a significant effect on predictions of cutting force. The instantaneous uncut chip thickness is estimated by following the movement of the position of the center of a cutter. To model analytically milling forces it is necessary to compute the chip volume and the specific cutting pressure. By the expression to uncut chip thickness proposed by (Kline & DeVor, 1983), the force model of end milling with cutter runout is established. This paper analyzes the behavior of the specific cutting pressures on end milling by calculating, from experimental data force, the pressure on each moment of cut considering the cutting force as much the edge force effect. Runout has been a limiting factor for achievable productivity in machining due to its adverse effects on tool life and part quality. The presence of cutter runout generates a cutting force component at the spindle rotational frequency and increases the average chip thickness for those teeth actually engaged in the cut. After the cutting pressure analysis some comparisons with previously published experiments by Yun & Cho (2001) will be done.

Keywords*. end milling , runout, uncut chip thickness, specific cutting force, machining modelling.*

1. Introduction

Cutter runout is a common phenomenon in multi-tooth machining operations, particularly in milling operations (Kline & DeVor, 1983). In end milling, runout commonly occurs due to cutter offset with respect to the spindle rotation when set screw-type holders are employed. Many other causes of cutter runout are possible, but in this paper, cutter offset with respect to the center of rotation is the type of runout considered.

The presence of runout causes chip load to vary over the rotation of a multi-tooth cutter. Depending on the degree and nature of runout, we can observe problems as cutter breakage, cutter wear, the surface error generation mechanism and the dynamic behavior of the machine tool and cutting process.

The cutting forces in end milling have often been considered as the product of a specific cutting force and uncut chip thickness (Araujo & Silveira, 1999, Yun & Cho, 2001). The uncut chip thickness can be separated into purely geometrical and physical aspects. The physical aspects of uncut chip thickness include the effects of cutter deflection, runout, vibration, and so forth.

2. Cutting force modelling of end milling operations

Instantaneous differential cutting force for one single flute was written by Martelotti (Tlusty & MacNeil, 1975):

$$d\vec{F}_{cutting} = \vec{K}_{cutting} \cdot t \cdot db \tag{1}$$

where t is the uncut chip thickness and db is a differential piece of the depth of cut.

And was rewritten by (Armarego, 1969) adding the edge parcel:

$$d\vec{F} = d\vec{F}_{edge} + d\vec{F}_{cutting} \tag{2}$$
$$d\vec{F} = \vec{K}_{edge} \cdot db + \vec{K}_{cutting} \cdot t \cdot db$$

where $\vec{K}_{edge}$ and $\vec{K}_{cutting}$ are vectors called specific edge pressure and specific cutting pressure, respectively.

The uncut chip thickness t for end milling is written as:

$$t = s_t \cdot sin(f) \tag{3}$$

where f is the angle of the cutting piece measured in relation of the normal direction of the feed per tooth s_t :

$$s_t = \frac{v}{w \cdot N_f} \tag{4}$$

from known v, w and N_f as the feed velocity, rotation velocity and the number of flutes.

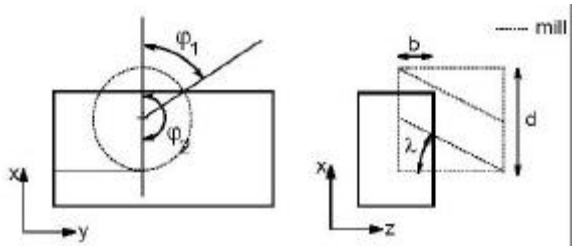

Figure 1. Milling geometry.

The cutting tool pieces can be calculated by

$$db = \frac{d}{2 \cdot \tan(l)} \cdot df \tag{5}$$

where d is the tool diameter and l is the helix angle, as shown in Fig. (1).

The angle d is calculated by

$$d = \frac{2 \cdot b \cdot \tan(l)}{d} \tag{6}$$

where b is the depth of cut and d is the contact angle.

The angle d is used to classify the cutting geometry as *Type I* or *Type II*,

$$\begin{aligned} &Type\ I \rightarrow d \le j_2 - j_1 \\ &Type\ II \rightarrow d > j_2 - j_1 \end{aligned} \tag{7}$$

where j_1 and j_2 are the entry and exit angles, respectively (Fig. (1)), enlightened on (Tlusty & MacNeil, 1975) and (Araujo & Silveira, 1999).

The force become:

$$\int \vec{K}_{edge} \cdot db + \int \vec{K}_{cutting} \cdot t \cdot db = \int \left(\vec{K}_{edge} + \vec{K}_{cutting} \cdot s_t \cdot sin(f)\right) \cdot \frac{d}{2 \cdot \tan(l)} \cdot df \tag{8}$$

So, the total force of cut, considering the N_f flutes of the mill, are calculated by the sum:

$$\vec{F} = \sum_{i=1}^{N_f} \vec{F}_i \tag{9}$$

In this approach, all force contributions are calculated at the same time because all differential parts of the force are calculated for each cutting piece.

The time variation of the milling force vector $\left(\vec{F}(t)\right)$ is written as the multiplication of functions in time.

$$\vec{F}(t) = \vec{K}_{edge}(t) \cdot h(t) + \vec{K}_{cutting}(t) \cdot A(t) \tag{10}$$

The specific forces, written as a vector function, ($\vec{K}_{edge}(t)$ and $\vec{K}_{cutting}(t)$), are multiplied by a scalar function relative to the height cutting ($h(t)$) and other relative to the cutting area, the scalar function ($A(t)$). This form is called from now on by *Functional approach*.

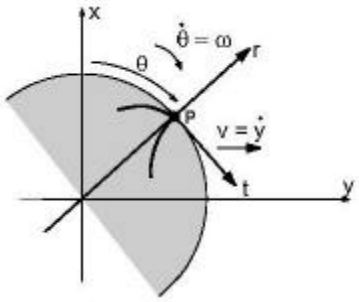

Figure 2. Milling tool referential.

The time variable t can be substituted by the angle of rotation q of a fixed point **P** in a peripheral tool and the tool velocity rotation w as shown in Fig. (2).

$$\vec{F}(t) = \tilde{\vec{F}}\left(\frac{q}{w}\right) = \vec{F}(q) \tag{11a}$$

$$\vec{F}(q) = \vec{K}_{edge}(q) \cdot h(q) + \vec{K}_{cutting}(q) \cdot A(q) \tag{11b}$$

The functions $h(q)$ and $A(q)$ will be calculated separately in the following sections.

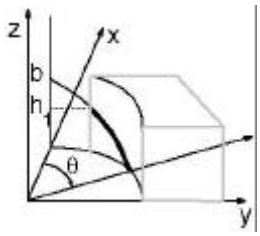

Figure 3. Height of cutting.

Table 1. Integration limits for each phase.

	Type I		Type II	
Phase	$L_1(\theta)$	$L_2(\theta)$	$L_1(\theta)$	$L_2(\theta)$
For $e_1 < \theta \leq e_2$ - Phase A	φ_1	θ	φ_1	θ
For $e_2 < \theta \leq e_3$ - Phase B	$\theta - \delta$	θ	φ_1	φ_2
For $e_3 < \theta \leq e_4$ - Phase C	$\theta - \delta$	φ_2	$\theta - \delta$	φ_2

3. The height function

In Fig. (3) can be observed the height of cutting of the first flute (h_1) at the milling angle q, for a cutting geometry.

The height function of cutting of the first flute $h_1(q)$ can be calculated by:

$$h_1(q) = \int_{L_1(q)}^{L_2(q)} \frac{d}{2 \cdot sin(l)} \cdot df \tag{12}$$

where the limits L_1 and L_2 are functions of q and are calculated differently for each cutting phase of q as can be observed on Table 1 and the values of e_1, e_2, e_3 and e_4 can be extracted from Tab. (2).

In order to add the contributions of all flutes, the height of cutting for any flute (n) is written by:

$$h_n(q) = \int_{L_1(q+x\cdot(n-1))}^{L_2(q+x\cdot(n-1))} \frac{d}{2 \cdot sin(l)} \cdot df \tag{13}$$

Note that the functions L_1 and L_2 are now not only a function of q but also a function of n, where x is the angle between the flutes.

Table 2. Variables values.

	Type I	Type II
e_1	φ_1	φ_1
e_2	$\varphi_1 + \delta$	φ_2
e_3	φ_2	$\varphi_1 + \delta$
e_4	$\varphi_2 + \delta$	$\varphi_2 + \delta$

The total height is calculated by:

$$h(q) = \sum_{n=1}^{N_f} h_n(q) \tag{14}$$

A height function of each flute, for a four flute tool, is present in Fig. (4).

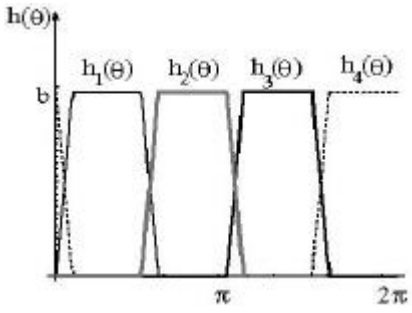

Figure 4. Function of height of cutting.

4. The cross-sectional area variation

In Fig. (5) can be observed the chip cross-sectional area (A_1) of the first flute at milling angle q, for a cutting geometry having $j_1 = 30°$ and $j_2 = p/2$.

The chip area can be calculated by:

$$A_1(q) = \int_{L_1(q)}^{L_2(q)} \frac{s_t \cdot sin(f) \cdot d}{2 \cdot sin(l)} \cdot df \tag{15}$$

where the limits L_1 and L_2 are functions of q and are calculated differently for each cutting phase of q as can be observed on Tab. (1).

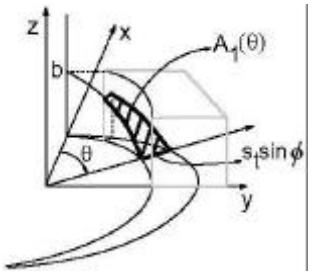

Figure 5. Chip cross-sectional area.

For a single flute and *Type I* cutting geometry, the chip cross-sectional area function is presented on Fig. (6). In order to add the contributions of all flutes, the chip cross-sectional area function for any flute (n) is written by:

$$A_n = \int_{L_1\cdot(q+x\cdot(n-1))}^{L_2\cdot(q+x\cdot(n-1))} \frac{s_t \cdot sin(f)\cdot d}{2\cdot sin(l)} \cdot df \tag{16}$$

Note that the functions L_1 and L_2 are now not only a function of q but also a function of n, where x is the angle between the flutes.

The total area is calculated by:

$$A(q) = \sum_{n=1}^{N_f} A_n(q) \tag{17}$$

and the Fig. (7) shows the chip cross-sectional area function $A(q)$ for a milling with four flutes $(x = 90°)$ and in bold the function of the first flute $A_1(q)$, of a cut having *Type I* geometry.

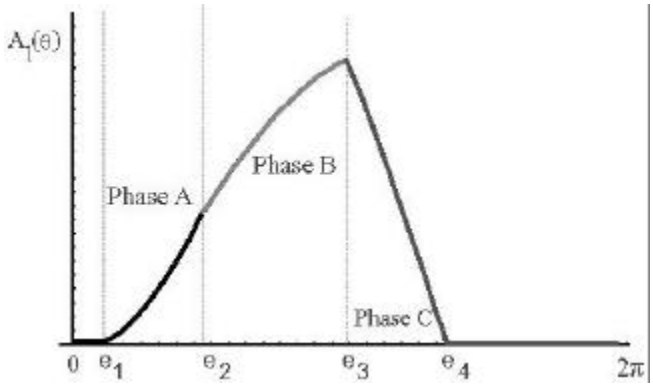

Figure 6. Area function for one single flute, without runout.

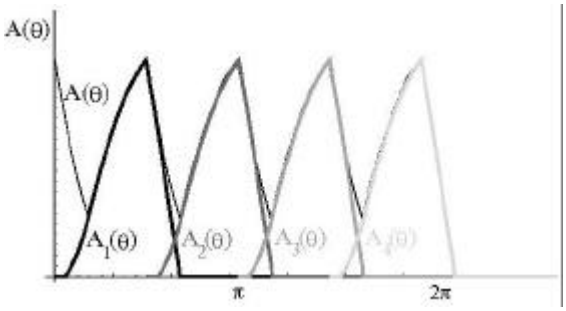

Figure 7. End milling area function, without runout.

5. Cutter runout

When runout is present, the uncut chip thickness (Eq. (3a)) must be modified to include the effect of the changing radius of the cutter teeth with respect to the axis of rotation.

Set screw-type tool holders commonly employed in industry to eliminate the problems of torsional and axial slippage of the cutter may induce cutter runout as the tightening action of the set screw tends to offset the cutter in the holder Fig. (8). As a result, the teeth on the offset side of the holder have a larger effective radius than do those on the other side of the cutter.

The position of the center of the cutter deviates from its nominal positions due to numerous factors, such as cutter deflection, runout, servo error, volumetric error, thermal error, wear, etc. Of all the factors, runout and cutter deflection account for the most deviation.

Cutter runout exists in all kinds of milling operations and results in variations in the uncut chip thickness, local forces and machined surface characteristics. The effect of runout is to redistribute the chip load among the flutes: the average chip thickness averaged over only the flutes engaged with the workpiece increases. The runout offset, r, can be easily measured by a dial gauge or other suitable device, whereas its location angle, e is difficult to measure. This angle determines the initial state of the predicted cutting forces. The uncut chip thickness in presence of runout is rewritten as: (Kline & DeVor, 1983).

$$t = s_t \cdot sin(f) + r \cdot \left(\cos(q - e - f) - \cos(q - e - f - n \cdot \frac{2 \cdot p}{N_f}) \right) \tag{3b}$$

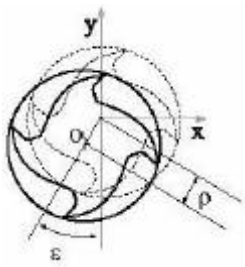

Figure 8. Cutter runout.

6. Force computation

In order to compare the present model with experimental data, the force components should be decomposed in x, y and z directions as they are usually recorded in machining tests.

$$\vec{F}(q) = \begin{bmatrix} F_x(q) \\ F_y(q) \\ F_z(q) \end{bmatrix} = A(q) \cdot \begin{bmatrix} K_{cx}(q) \\ K_{cy}(q) \\ K_{cz}(q) \end{bmatrix} + h(q) \cdot \begin{bmatrix} K_{ex}(q) \\ K_{ey}(q) \\ K_{ez}(q) \end{bmatrix} \tag{18}$$

But it's not convenient to write the specific cutting force in the fixed referential *x, y, z*. To rewrite it on the more appropriate tool referential *t, r, z* (tangential, radial and axial directions), another functions $A_R(q)$ and $h_R(q)$ has to be introduced:

$$\begin{bmatrix} F_x(q) \\ F_y(q) \\ F_z(q) \end{bmatrix} = A_R(q) \cdot \begin{bmatrix} K_{ct}(q) \\ K_{cr}(q) \\ K_{cz}(q) \end{bmatrix} + h_R(q) \cdot \begin{bmatrix} K_{et}(q) \\ K_{er}(q) \\ K_{ez}(q) \end{bmatrix} \tag{19}$$

In fact, the function $A_R(q)$ and $h_R(q)$ are the rotation matrix $R(q)$ multiplied by the area and the height, respectively.

$$R(q) = \begin{pmatrix} \cos(q) & sin(q) & 0 \\ sin(q) & -\cos(q) & 0 \\ 0 & 0 & 1 \end{pmatrix} \tag{20}$$

The rotation matrix $R_n(q)$ have to be written for each flute:

$$R_n(q) = \begin{pmatrix} \cos(q + x \cdot (n-1)) & sin(q + x \cdot (n-1)) & 0 \\ sin(q + x \cdot (n-1)) & -\cos(q + x \cdot (n-1)) & 0 \\ 0 & 0 & 1 \end{pmatrix} \tag{21}$$

Then, for all flutes, the rotated area function becomes:

$$A_R(q) = \sum_{n=1}^{N_f} R_n(q) \cdot A_n(q) \tag{22}$$

and the rotated height function is:

$$h_R(q) = \sum_{n=1}^{N_f} R_n(q) \cdot h_n(q) \tag{23}$$

To simplify the following calculations, $S_1(q)$, $S_2(q)$, $S_3(q)$ and $S_4(q)$ are defined:

$$S_1(q) = \sum_{n=1}^{N_f} A_n(q) \cdot \cos(q + x \cdot (n-1)) \tag{24a}$$

$$S_2(q) = \sum_{n=1}^{N_f} A_n(q) \cdot sin(q + x \cdot (n-1)) \tag{24b}$$

$$S_3(q) = \sum_{n=1}^{N_f} h_n(q) \cdot \cos(q + x \cdot (n-1)) \tag{24c}$$

$$S_4(q) = \sum_{n=1}^{N_f} h_n(q) \cdot sin(q + x \cdot (n-1)) \tag{24d}$$

Rewriting the Eq. (19), the force can be expressed by:

$$\begin{bmatrix} F_x(q) \\ F_y(q) \\ F_z(q) \end{bmatrix} = A_R(q) \cdot \begin{bmatrix} K_{ct}(q) \\ K_{cr}(q) \\ K_{cz}(q) \end{bmatrix} + h_R(q) \cdot \begin{bmatrix} K_{et}(q) \\ K_{er}(q) \\ K_{ez}(q) \end{bmatrix} \tag{25a}$$

$$\begin{bmatrix} F_x(q) \\ F_y(q) \\ F_z(q) \end{bmatrix} = \begin{bmatrix} S_1(q) & S_2(q) & 0 & S_3(q) & S_4(q) & 0 \\ S_2(q) & -S_1(q) & 0 & S_4(q) & -S_3(q) & 0 \\ 0 & 0 & A(q) & 0 & 0 & h(q) \end{bmatrix} \cdot \begin{bmatrix} K_{ct}(q) \\ K_{cr}(q) \\ K_{cz}(q) \\ K_{et}(q) \\ K_{er}(q) \\ K_{ez}(q) \end{bmatrix} \tag{25b}$$

Note that the matrix $J(q)$ is the Jacobian of the **F** components in relation to the specific cutting pressure coefficients.

$$J(q) = \begin{bmatrix} S_1(q) & S_2(q) & 0 & S_3(q) & S_4(q) & 0 \\ S_2(q) & -S_1(q) & 0 & S_4(q) & -S_3(q) & 0 \\ 0 & 0 & A(q) & 0 & 0 & h(q) \end{bmatrix} = \begin{bmatrix} \frac{\partial F_x}{\partial K_{ct}} & \frac{\partial F_x}{\partial K_{cr}} & \frac{\partial F_x}{\partial K_{cz}} & \frac{\partial F_x}{\partial K_{et}} & \frac{\partial F_x}{\partial K_{er}} & \frac{\partial F_x}{\partial K_{ez}} \\ \frac{\partial F_y}{\partial K_{ct}} & \frac{\partial F_y}{\partial K_{cr}} & \frac{\partial F_y}{\partial K_{cz}} & \frac{\partial F_y}{\partial K_{et}} & \frac{\partial F_y}{\partial K_{er}} & \frac{\partial F_y}{\partial K_{ez}} \\ \frac{\partial F_z}{\partial K_{ct}} & \frac{\partial F_z}{\partial K_{cr}} & \frac{\partial F_z}{\partial K_{cz}} & \frac{\partial F_z}{\partial K_{et}} & \frac{\partial F_z}{\partial K_{er}} & \frac{\partial F_z}{\partial K_{ez}} \end{bmatrix} \tag{26}$$

7. Specific force analysis

The problem is concentrated on the specific force analysis. The Eq. (25) can be easily calculated if the specific pressures are constant in q.

Kline & DeVor (1983) assumed that the specific cutting forces are functions of cutting conditions, and the values were calculated using the average cutting forces during one revolution of a cutter.

If parameters of orthogonal and oblique models are time constant, the specific cutting force do not change in time. To analyze this behavior, for each point of q, the equation:

$$K(q) = \frac{1}{2} \cdot \left(J^{-1}(q - dq) \cdot F(q - dq) + J^{-1}(q + dq) \cdot F(q + dq) \right) \tag{27}$$

The shown experimental cutting force data in the Fig. (9) had been extracted of the article (Yun & Cho, 2001, p.476, Fig. (8c)) and previously had been synchronized and adequately adjusted for the execution of the analysis. Yun and Cho (2001) test cuts were performed with high-speed steel (HSS) end mills with four flutes, 30° helix angle, 11° rake angle and 10 mm diameter in a vertical type machining center. The workpiece material was aluminum 2014-T6. A tool dynamometer (Kistler, type 9257B) was used to measure the three cutting force components. The experiment performed by Yun and Cho and used in this work has the following parameters:

$d = 10mm$, $l = 30°$, $N_f = 4$, $b = 2mm$, $j_1 = 0$, $j_2 = \frac{p}{2}$, $s_t = 0.0375mm/tooth$

$\left\{ \begin{matrix} r = 0.0084mm \\ e = 211° \end{matrix} \right\}$ → Estimated values by the authors of this paper, after the analysis of the experimental cutting force data.

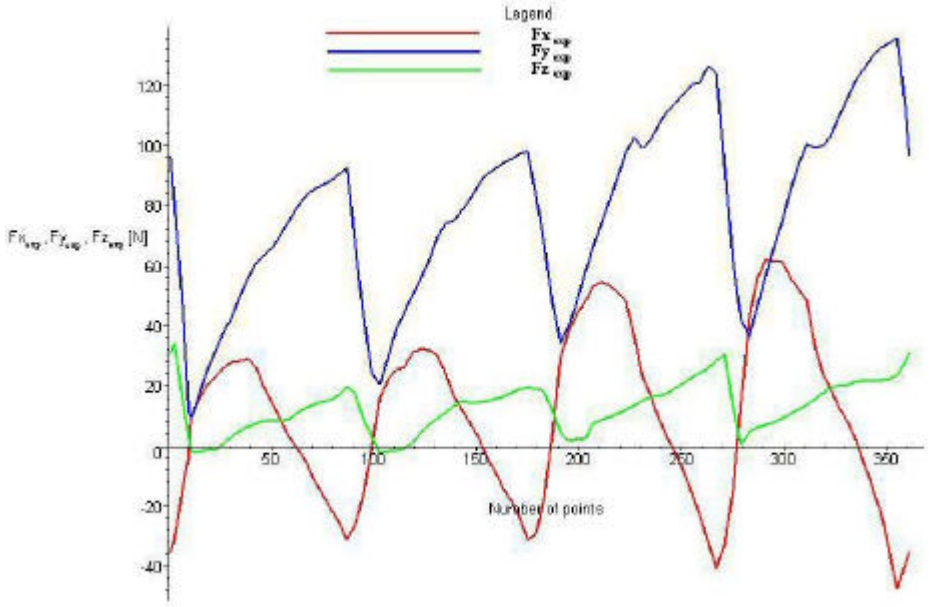

Figure 9. Experimental data from (Yun & Cho, 2001, p.476, Fig. (8c)).

But, when calculating the Eq. (27), appears a singularity because there are three parameters and six unknown variables. To solve this problem, we suppose that two consecutive points have the same specific force, calculating the specific force for each interval:

$$\begin{bmatrix} F_x(q) \\ F_y(q) \\ F_z(q) \\ F_x(q+dq) \\ F_y(q+dq) \\ F_z(q+dq) \end{bmatrix} = J_A(q) \cdot \begin{bmatrix} K_{ct}(q) \\ K_{cr}(q) \\ K_{cz}(q) \\ K_{et}(q) \\ K_{er}(q) \\ K_{ez}(q) \end{bmatrix} \tag{28}$$

The matrix J amplified became a square matrix J_A:

$$J_A = \begin{bmatrix} S_1(q) & S_2(q) & 0 & S_3(q) & S_4(q) & 0 \\ S_2(q) & -S_1(q) & 0 & S_4(q) & -S_3(q) & 0 \\ 0 & 0 & A(q) & 0 & 0 & h(q) \\ S_1(q+dq) & S_2(q+dq) & 0 & S_3(q+dq) & S_4(q+dq) & 0 \\ S_2(q+dq) & -S_1(q+dq) & 0 & S_4(q+dq) & -S_3(q+dq) & 0 \\ 0 & 0 & A(q+dq) & 0 & 0 & h(q+dq) \end{bmatrix} \tag{29}$$

and the problem has only one solution:

$$\begin{bmatrix} K_{ct}(q) \\ K_{cr}(q) \\ K_{cz}(q) \\ K_{et}(q) \\ K_{er}(q) \\ K_{ez}(q) \end{bmatrix} = \frac{1}{2} \cdot \left(\left[J_A(q-dq) \right]^{-1} \cdot \begin{bmatrix} F_x(q-dq) \\ F_y(q-dq) \\ F_z(q-dq) \\ F_x(q) \\ F_y(q) \\ F_z(q) \end{bmatrix} + \left[J_A(q+dq) \right]^{-1} \cdot \begin{bmatrix} F_x(q+dq) \\ F_y(q+dq) \\ F_z(q+dq) \\ F_x(q+2 \cdot dq) \\ F_y(q+2 \cdot dq) \\ F_z(q+2 \cdot dq) \end{bmatrix} \right) \tag{30}$$

Calculating the best "average" value of the specific values obtained for hole rotation $\overline{K}$, and applying on Eq. (25) results:

$$\begin{bmatrix} F_x(q) \\ F_y(q) \\ F_z(q) \end{bmatrix} = J(q) \cdot \begin{bmatrix} \overline{K}_{ct} \\ \overline{K}_{cr} \\ \overline{K}_{cz} \\ \overline{K}_{et} \\ \overline{K}_{er} \\ \overline{K}_{ez} \end{bmatrix} \tag{31}$$

as shown in Tab. (3).

Table 3. Average specific pressures values.

$\overline{K}_{ct}$ [N/mm^2]	$\overline{K}_{cr}$ [N/mm^2]	$\overline{K}_{cz}$ [N/mm^2]	$\overline{K}_{et}$ [N/mm]	$\overline{K}_{er}$ [N/mm]	$\overline{K}_{ez}$ [N/mm]
918.81	-283.52	273.16	9.55	-9.49	-1.97

Using these values to recalculate the forces, Fig. (10), Fig. (11) and Fig. (12) for Fx, Fy and Fz respectively, shows the comparison between experimental force and semi-empirical force. This procedure aims to confirm if the behavior of the specific pressure considered is correct.

8. Conclusions

This paper analyzes the behavior of the specific cutting pressures from experimental cutting force data. A procedure to estimate the specific cutting forces from data is developed using the function approach including the edge parcel and the runout parameters in the model. The method is validated by recalculation of the cutting force and compared with the experiment published by (Yun & Cho, 2001). After the analysis of the results, it's evident that the proposed model is effective and accurate. In order to improve the model, the cutter deflection need to be added.

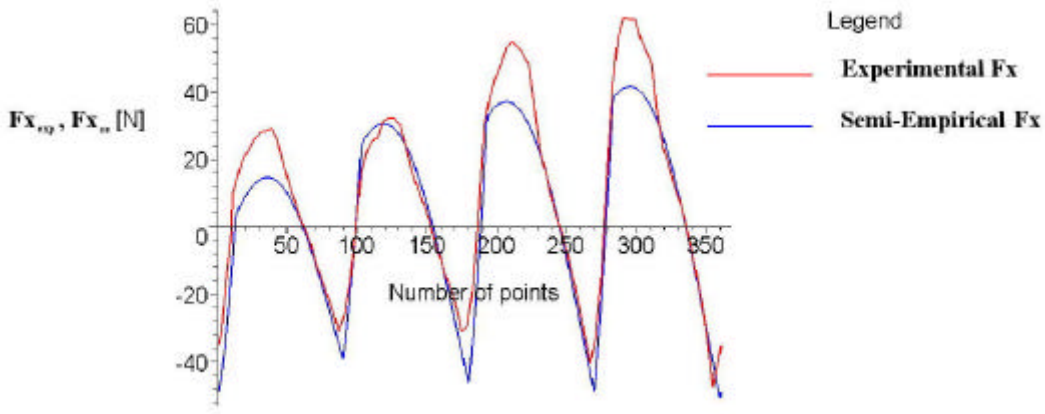

Figure 10. Comparison between the experimental F_x and the semi-empirical F_x.

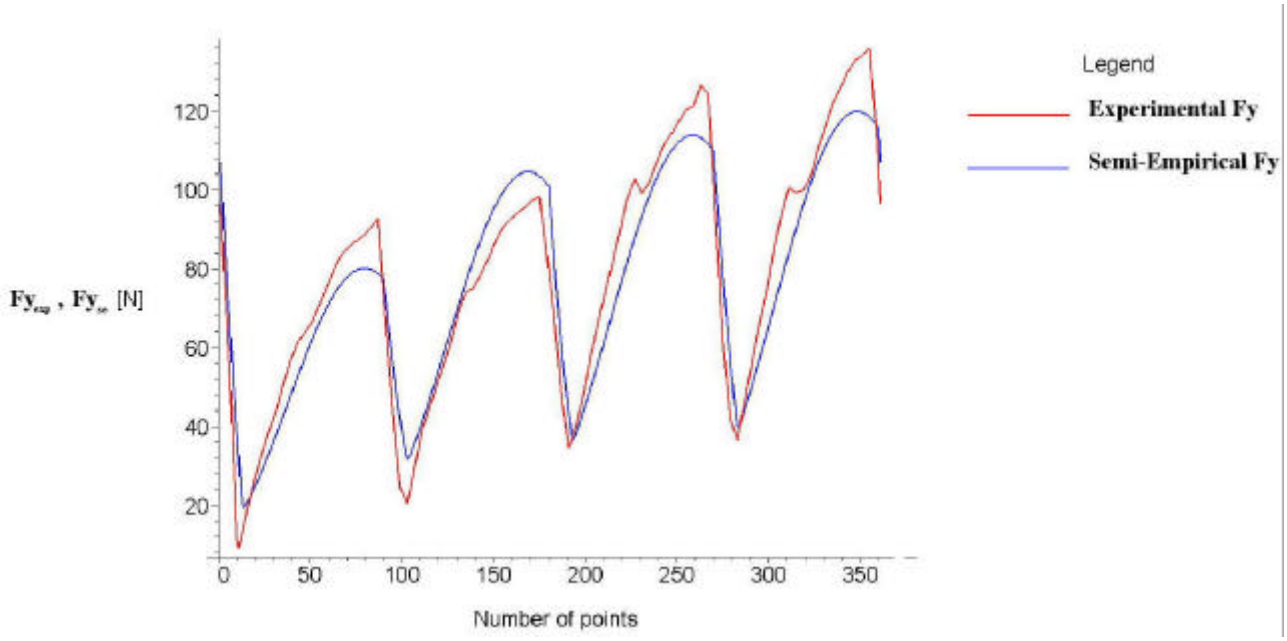

Figure 11. Comparison between the experimental F_y and the semi-empirical F_y.

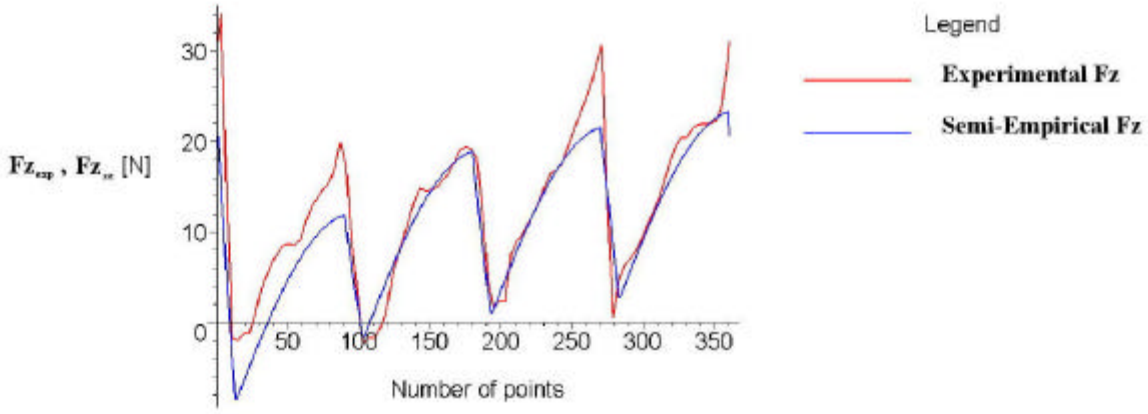

Figure 12. Comparison between the experimental F_z and the semi-empirical F_z.

9. Acknowledgements

This project was stimulated through the fellowship received from the CAPES (Coordenação de Aperfeiçoamento de Pessoal de Nível Superior) of Brazil. The authors are grateful to this entity and also the Federal University of Rio de Janeiro for the support.

10. References

Araujo, A.C. & Silveira, J.L., 1999, "Models for the Prediction of Instantaneous Cutting Forces in End Milling", Annals of 15th COBEM, CDROM.

Araujo, A.C. & Silveira, J.L., 2001, "Analysis of the Specific force on End Milling", Proceedings of the 22nd Iberian Latin-American Congress on Computational Methods in Engineering, Campinas, SP, Brazil.

Armarego, E. & Brown, J., 1969, "The Machining of Metals", Prentice-Hall, New Jersey.

Kline, W.A. & DeVor, R.E., 1983, 'The Effect of Runout on Cutting Geometry and Forces in End Milling", Int. J. of Machine Tool Design and Research, vol. 23, No.2/3, pp. 123-140.

Tlusty, J. & MacNeil, P., 1975, "Dynamics of Cutting in End Milling", Annals of the CIRP, vol. 24/1, pp. 213-221.

Yun, W.S. & Cho, D.W., 2001, "Accurate 3-D Cutting Force Prediction using Cutting Condition Independent Coefficients in End Milling", Int. J. Mach. Tool Man., vol. 41, pp. 463-478.